

PROGRESS IN 3D SELF-CONSISTENT FULL WAVE-PIC MODELLING OF SPACE RESOLVED ECR PLASMA PROPERTIES

A. Pidotella*, G. S. Mauro, B. Mishra, E. Naselli, G. Torrioni, D. Mascali

Istituto Nazionale di Fisica Nucleare - Laboratori Nazionali del Sud, Catania, Italy

A. Galatà, C. S. Gallo

Istituto Nazionale di Fisica Nucleare - Laboratori Nazionali di Legnaro, Legnaro, Italy

Abstract

We present updates of a simulation suite to model in-plasma ion-electron dynamics, including self-consistent electromagnetic (EM) wave propagation and population kinetics to study atomic processes in ECR plasmas. The EM absorption is modelled by a heuristic collisional term in the cold dielectric tensor. The tool calculates steady-state particle distributions via a full-wave Particle-In-Cell code and solves for collisional-radiative process giving atomic and charge state distributions (CSD). The scheme is general and applicable to many physics' cases of interest for the ECRIS community, including the build-up of the CSD and the plasma emitted X-ray and optical radiation. We present the code's last updates and future perspectives, using as a case-study the PANDORA scenario. We report about studying in-plasma dynamics of injected metallic species and radioisotopes ionisation efficiencies for different injection conditions and plasma parameters. The code is capable of reconstructing space-resolved plasma emissivity comparable to measurements and modelling plasma-induced modification of radioactivity.

INTRODUCTION

Electron cyclotron resonance ion sources (ECRIS) are widely used in accelerator facilities around the world to provide high current ion beams with charge states tuned according to experimental requirements. They operate on the dual concept of resonance heating with microwaves and magnetic confinement using a min-B profile that generates a compact and dense plasma composed of energetic electrons and multi-charged ions. In a complementary way, ECR ion trap can be also serve as a facility resembling stellar plasma conditions, useful for performing interdisciplinary experiments interesting for nuclear physics, atomic physics and astrophysics [1]. While operational ECRIS are often designed using empirical scaling laws [2], the physics of plasma leading the ion generation process as well as the charged particles' dynamics in it is really intricate due to the multi-physics interactions between static and dynamic electromagnetic fields and particles. Simulations are a powerful tool to investigate the microscopic structure of ECR plasma and improve our fundamental understanding of these devices thereof. In the following, various aspects of space-resolved 3D full-wave Particle-In-Cell (PIC) model developed to study the ECR plasma properties and therein particle interactions are pre-

sented in detail. The description of the code will follow a schematic simulation pipeline: a first-level high-precision input given in terms of steady-state electrons distributions in the simulation domain; in cascade, a second-level input will be given by computing steady-state ion charge distribution in plasma imposed by the pre-simulated electron dynamics; finally, external neutral/charged particles interaction with the electron/ion distributions is studied aiming at reconstructing their in-plasma reactions.

PLASMA ELECTRONS DYNAMIC SIMULATIONS

The ground level of the 3D full-wave electron PIC code is a set of routines employing MATLAB[®] as a particle pusher and COMSOL Multiphysics[®] as a FEM solver to generate 3D profiles of electron density (n_e) and average energy (E_e) self-consistent with EM field distribution [3, 4]. The electrons simulation implies a looped scheme where initial macro-particles are first moved and energised by the EM field distribution of the microwaves injected into the vacuum chamber, generating a first density profile based on the dielectric tensor treatment in *cold* plasma approximation. Then, fields are recalculated based on the updated electron density, including long-range Coulomb collisions for catching both particles' deterministic frictions and random diffusion, till convergence between the particle and field profiles is reached. A flowchart representing the simulation scheme is shown in Fig. 1(a). The algorithm has been applied to various types of ECRIS configurations [5–8], and is an excellent tool to produce space- and energy-resolved distributions of n_e and E_e . Figure 1(b-c) shows a comparison of E_e obtained from the simulations of a 14.28 GHz, 200 W ECRIS operational at ATOMKI, Debrecen and of a 14.428 GHz, 100 W ECRIS operations at INFN-LNL, Legnaro, hereafter LEGIS. In both ECRIS distributions are strongly space-dependent, owing to differences in shape and size of the plasma chamber, microwave frequency and power. The data in these plots represent the source maps which form the basis of ion dynamics calculations. We have recently attempted to overcome the *cold* plasma approximation in the EM wave damping in plasma. Preliminary results of the developed 1D semi-analytical model of EM wave propagation including a *hot* tensor plasma response have been presented. The study allowed to investigate on the coupling of antenna-generated 60 MHz fast X-waves to realistic plasma fusion scenario within the Divertor Tokamak Test (DTT) project. Considering linearised Vlasov-Maxwell equations, stationary and

* pidotella@lns.infn.it

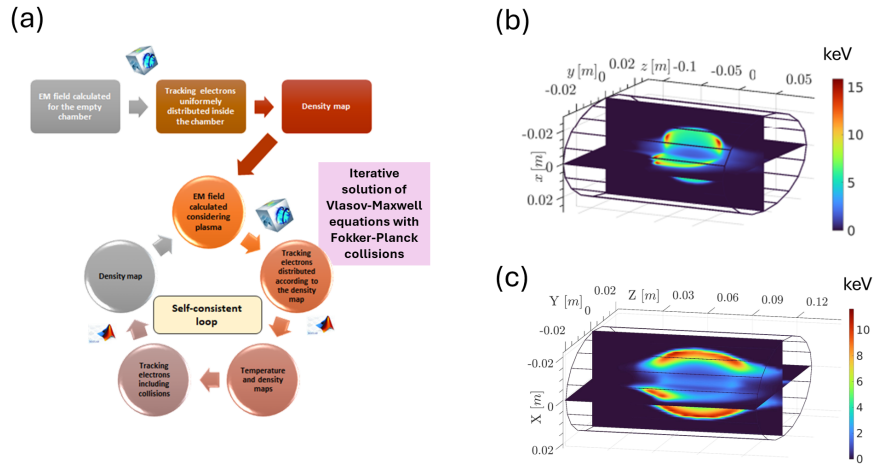


Figure 1: Schematic PIC loop for electrons (a). Electron mean energy [keV] 3D distributions for the ATOMKI ECRIS (Debrecen, Hungary) at 14.28 GHz and 200 W of RF power (b) and the LEGIS ECRIS (Legnaro, Italy) at 14.428 GHz and 100 W of RF power (c).

homogeneous plasma, with no strong EM perturbations, and in a collision-less scenario, we could model the electron Landau damping of the wave imposed by the expected plasma profile. Details can be found in Ref. [9]. Efforts to adapt the hot tensor description in ECR plasma-based devices are ongoing.

PLASMA IONS DYNAMIC SIMULATIONS

The second level of simulations allows to model ECR plasma ions properties using a PIC Monte Carlo (MC) code which takes as input steady state n_e and E_e maps from electron PIC outputs to compute the corresponding steady-state ion maps, based on the following ion balance equation:

$$\frac{\dot{n}_i}{n_e} = n_{i-1}\gamma_{i-1,i} - n_i\gamma_{i,i+1} + n_{i+1}nE_{i+1,i} - n_i nE_{i,i-1} - \frac{n_i}{n_e\tau_i},$$

with n_i the ion number density of charge state i , γ the electron impact (EI) ionisation rate, $n = n_0/n_e$ the neutral gas over electron density ratio, E the single-electron charge exchange (CEX) rate, and τ_i the characteristic confinement time of the charge state.

The flowchart representing the PIC-MC simulation scheme is shown in Fig. 2. For each charge state i , N representative macro-particles are sampled according to an ionisation map and moved in a collisional plasma. During their transport, EI and CEX ionisation are considered via MC routine, and the trajectories of remaining particles mapped to occupation maps. At intermediate time steps, accumulated maps are extracted, properly scaled to charge density maps, solving via the Poisson equation for the local charge unbalance imposed by the self-built up electron and charge-state distribution (CSD). The solution will provide the self-generated electric potential map, thus the related electrostatic field components acting to equilibrate the charge unbalance and serving to the formation of the well-known *double-layer* (DL) confinement close to the ECR surface. At the end of the PIC simulation for each i , occupation maps are converted into density maps using charge neutrality and

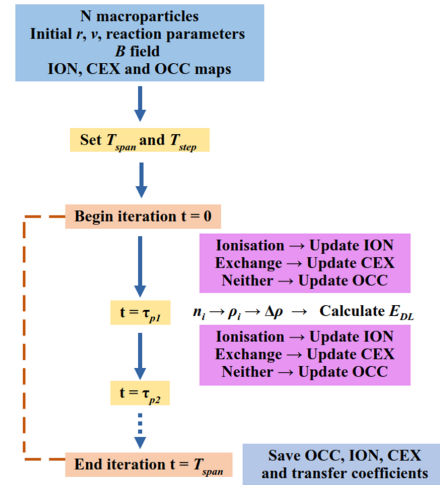


Figure 2: Schematic of PIC-MC loop for ions.

a proper scaling accounting for all the forward (backward) atomic processes in the CSD built-up.

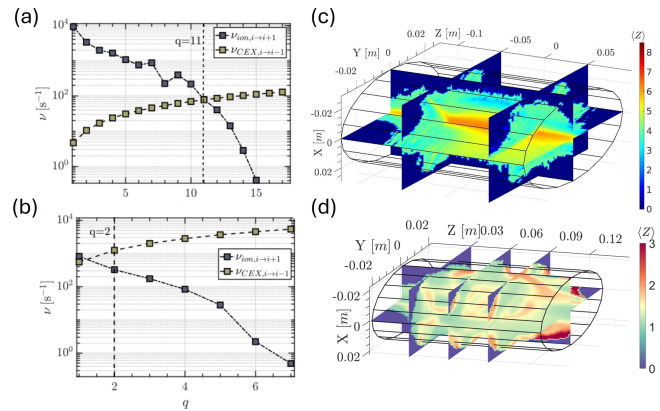


Figure 3: Volume averaged reaction frequencies for EI and CEX process as function of the charge state q for ATOMKI (a) and Legnaro (b) ECRIS. Mean charge distributions for Argon (c) and Oxygen (d) buffer ions in ATOMKI and Legnaro, respectively.

This allows to generate the CSD which converges to the true steady-state value as more charge states are simulated. An example of the utility of the PIC-MC code can be seen in Fig. 3(a-b) which shows the EI/CEX average reaction frequencies vs. q charge state for Ar (O) buffer ions for ATOMKI (LEGIS) ECR sources, respectively, corresponding to E_e shown in Fig. 1(b-c). Not only the different gas species plays a role in a different trend of reactions as a function of q , but also the different operative conditions (RF power, gas pressure, geometry, frequency) impact on the q where one of the processes overcomes the other. Such predictions might help ECRIS operators in fine-tuning the CSD accordingly to the expected atomic physics occurring in plasma. In Fig. 3(c-d) the different mean-charge distributions are shown for ATOMKI and LEGIS, respectively. More details on the algorithm, its various components and conclusive results are present in Ref. [4]. Experimental benchmark of the ion dynamics from PIC-MC simulations can be provided by comparing the predicted ion current as a function of charge state (current profile) with its counterpart read at the Faraday cup. The ion density n_i is the given input, then the simulated extracted current is given by:

$$I_i = \kappa \frac{LS \langle n_i \rangle q_i e}{\tau_i}, \quad (1)$$

with κ the transmission factor, L is the semi-plasma length and S is the area of the extraction hole. A critical parameter in Eq. (1) is the confinement time τ_i given as the reciprocal sum of *ambipolar diffusion* and *electrostatic confinement* time. The latter arises from the electrostatic DL

the current profile extracted from the ATOMKI ECRIS and that simulated using the PIC-MC code and Eq. (1). As can be observed, the general trends and overall magnitude of the current are decently reproduced only if the electrostatic confinement (in Fig. 4(b) is included in the confinement time, underlining the reliability of the model usable to predict ion beam currents in other ECRIS designs.

IN-PLASMA DYNAMICS OF INJECTED RADIOISOTOPES: STUDY OF IONISATION AND NUCLEAR DECAY RATES

In the upcoming years a new facility currently under construction at the INFN-LNS in Catania, Italy, will be available to perform in-plasma inter-disciplinary experiments. The PANDORA facility [1] aims to use a compact and high-energy density ECR magnetoplasma as a stellar emulator for in-plasma measurement of nuclear decay rates and heavy element opacity. Both these quantities depend on ion CSD and electron properties [11, 12] and which are expected to vary strongly in the plasma. Here we present two applications of interest for the PANDORA physics cases of the PIC-MC simulation tool described in the previous sections. Plasma-induced decay rate modification is a cornerstone of the PANDORA facility. In-plasma β -decay rates are given by $\lambda^* = (\ln 2 / ft) f^*$ where ft is related to the nuclear matrix element of the decay, according to the Fermi theory of the nuclear decay, and f^* is the lepton phase volume calculated in the plasma. Accordingly to Ref. [11], the in-plasma decay rate can be strongly influenced by the presence of empty atomic inner shells, entering in the so-called *bound-state* β decays (e^- emitted in a bound free shell) or decaying via *orbital electron capture* (picking up e^- from bound electrons in the inner shells).

Such dependency is therefore strongly connected to the in-plasma CSD and atomic level population, biased by the thermodynamics of the radioactive isotope in plasma and the ongoing atomic processes (ionisations and excitations). The probability distribution of the radioactive ions in the plasma and can be calculated using the ion PIC-MC code with an extended balance equation including all collisional and radiative processes [13]. The application of this method can be seen in Fig. 5(c-d) which shows the ^7Be mean-charge distribution following the ionisation dynamics after injection of $^7\text{Be}^{1+}$ in the LEGIS plasma oxygen at 5×10^{-5} mbar pressure (c) and the related 3D variation (up to 50 %) in the electron capture half-life $t_{1/2}$ of ^7Be ions (terrestrial $t_{1/2} \sim 55$ days), as expected from theoretical calculations [14]. The ^7Be decay into ^7Li via electron capture is one of the PANDORA physics cases, interesting for the cosmological lithium problem and for its impact on the primordial nucleosynthesis. Another interesting case is the ^{134}Cs isotope (terrestrial $t_{1/2} \sim 2$ years), as being a key nuclei in a branching point of s -process nucleosynthesis in massive stars. Its β^- -decay rate change in plasma could be observed in PANDORA via a dedicated HPGe detectors

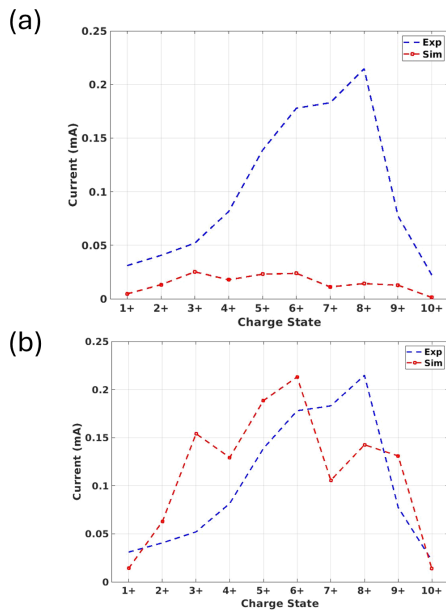


Figure 4: Experimental vs. simulated extracted ion beam current for the ATOMKI ECRIS, including only ambipolar diffusion (a) or both ambipolar and electrostatic confinement (b).

self-generated in the PIC-MC simulation and predicted to exist in ECR plasma [10]. Figure 4 shows a comparison of

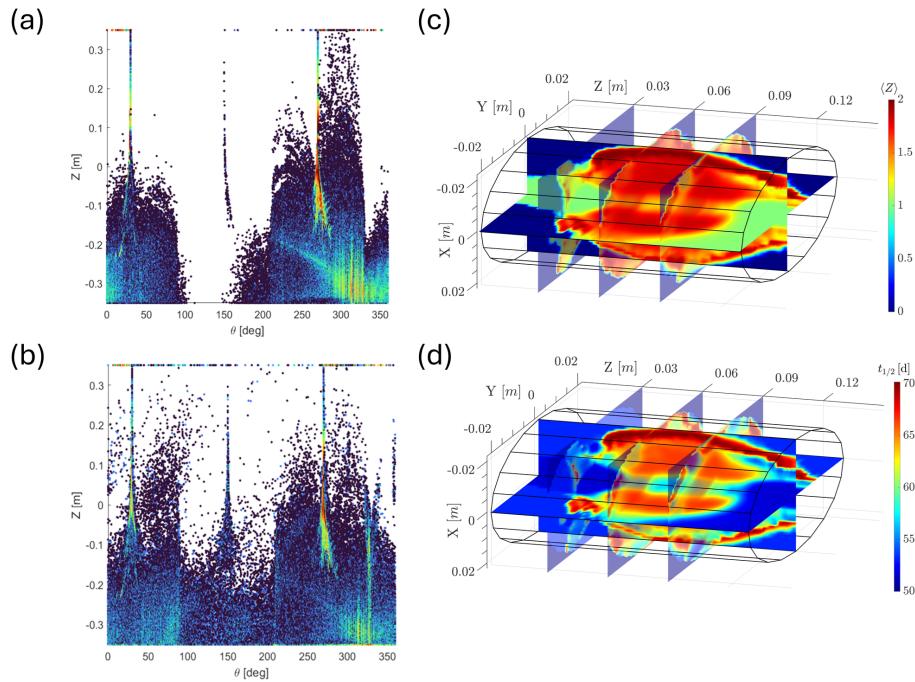


Figure 5: Deposition rate maps of caesium isotope (^{134}Cs) thermal evaporation (420 K) via resistively heated ovens and after in-plasma ionisation, with (a) and without (b) hot screen (liner, simulated at 800 K) at the plasma chamber wall. Mean-charge distribution of ^7Be in the plasma trap following $^7\text{Be}^{1+}$ injection (c) and related half-life time accordingly to the in-plasma nuclear decay modelling in Ref. [14].

array surrounding the trap, looking for the daughter nuclei EM de-excitation via γ emission. However, the γ signal arising from the decay in plasma must be disentangled from the overwhelming γ noise self-generated by the plasma and Bremsstrahlung emission. Moreover, neutral isotopes condensing at the cold plasma chamber wall decay too, and such signal represents an additional source of noise to the detection system. A MC simulation has been recently performed looking at the dynamics of injected Cs particles in plasma via thermal evaporation, studying the ionisation efficiency of the PANDORA non-axisymmetric injection system and at the same time the expected amount of depositing neutral metallic atoms. The latter aspect turned to be useful in estimating the γ noise arising from the Cs deposition at the wall in the detection system [15]. In Fig. 5(a-b) the deposition maps at the PANDORA chamber wall (unfolded in the longitudinal z -axis and azimuth θ coordinates) are shown, where the recycling effects of low-melting Cs imposed by the usage of a hot screen (b) is contrasted to the case where no hot screen is used (a). The results underline the relevant role played by the plasma and magnetic field in the isotope dynamics.

CONCLUSION

This paper presented an outline of coupled 3D full-wave PIC and PIC-MC codes capable of describing space-resolved properties of electrons and ions in an ECR plasma self-consistently. The results of the simulations are fundamental inputs to various physical processes, which can be used to validate the models while simultaneously underlining their

predictive power. The simulation schemes are currently being updated in various ways including substitution of the cold electron approximation with the corrected hot electron dielectric tensor, addition of more reactions and improvement of previous ones for better modelling of ion dynamics and full implementation of the collision-radiative model for NLTE plasma-induced decay rate evaluation. The updated simulations will be compared with suitable experimental data from other ECRIS and the results will be reported in future works.

ACKNOWLEDGEMENTS

The authors acknowledge the financial support from the MUR-PNRR project PE0000023-NQSTI and the MUR-PNRR project SAMOTHRACE (ECS00000022), financed by the European Union (NextGeneration EU). The authors also wish to thank INFN for the support through the project PANDORA Gr3 funded by third Nat. Sci. Comm.

REFERENCES

- [1] D. Mascali *et al.*, “A Novel Approach to β -Decay: PANDORA, a New Experimental Setup for Future In-Plasma Measurements”, *Universe*, vol. 8, p. 80, 2022. doi:10.3390/universe8020080
- [2] R. Geller, *Electron cyclotron resonance ion sources and ECR plasmas*, Institute of Physics, Bristol, UK, 2018.
- [3] D. Mascali *et al.*, “3D-full wave and kinetics numerical modelling of electron cyclotron resonance ion sources plasma: steps towards self-consistency”, *Eur. Phys. J. D*, vol. 69, p. 27, 2015. doi:10.1140/epjd/e2014-50168-5

- [4] B. Mishra *et al.*, “Modeling space-resolved ion dynamics in ECR plasmas for predicting in-plasma β -decay rates”, *Front. Phys.*, vol. 10, p. 932448, 2022. doi:10.3389/fphy.2022.932448
- [5] A. Galatà *et al.*, “On the Numerical Determination of the Density and Energy Spatial Distributions relevant for in-Plasma β -Decay Emission Estimation”, *Front. Phys.*, vol. 10, p. 947194, 2022. doi:10.3389/fphy.2022.947194
- [6] A. Galatà *et al.*, “Self-consistent modeling of beam-plasma interaction in the charge breeding optimization process”, *Rev. Sci. Instrum.*, vol. 91, p. 013506, 2020. doi:10.1063/1.5130704
- [7] R. Rácz *et al.*, “Electron cyclotron resonance ion source plasma characterization by energy dispersive x-ray imaging”, *Plasma Sources Sci. Technol.*, vol. 26, p. 075011, 2017. doi:10.1088/1361-6595/aa758f
- [8] A. Galatà *et al.*, “A new numerical description of the interaction of an ion beam with a magnetized plasma in an ECR-based charge breeding device”, *Plasma Sources Sci. Technol.*, vol. 25, p. 045007, 2016. doi:10.1088/0963-0252/25/4/045007
- [9] C. Salvia *et al.*, “Simulations of RF waves propagation in hot magnetized (^2H) plasma in DTT Scenario”, *Il Nuovo Cimento C*, no. 5, p. 271, 2024. doi:10.1393/ncc/i2024-24271-0.
- [10] D. Mascali *et al.*, “A double-layer based model of ion confinement in electron cyclotron resonance ion source”, *Rev. Sci. Instrum.*, vol. 85, p. 02A511, 2014. doi:10.1063/1.4860652
- [11] K. Takahashi and K. Yokoi, “Nuclear β -decays of highly ionized heavy atoms in stellar interiors”, *Nucl. Phys. A.*, vol. 404, p. 3, 1983. doi:10.1016/0375-9474(83)90277-4
- [12] A. Pidotella *et al.*, “Angelo Pidotella [HTML] da frontiersin.org Experimental and numerical investigation of magneto-plasma optical properties towards measurements of opacity relevant for compact binary objects”, *Front. Astron. Space Sci.*, vol. 9, p. 225, 2022. doi:10.3389/fspas.2022.931744
- [13] B. Mishra, “Overview of Numerical Simulations for Calculating In-Plasma β -Decay Rates in the Framework of PANDORA Project”, *Eur. Phys. J. Web Conf.*, vol. 275, p. 02001, 2023. doi:10.1051/epjconf/202327502001
- [14] B. Mishra *et al.*, “Plasma Induced Variation of Electron Capture and Bound-State β Decays”, *arXiv*, 2024. doi:10.48550/arXiv.2407.01787
- [15] A. Pidotella *et al.*, “Metal evaporation dynamics in electron cyclotron resonance ion sources: plasma role in the atom diffusion, ionisation, and transport”, *Plasma Phys. Control. Fusion*, vol. 66, p. 035016, 2024. doi:10.1088/1361-6587/ad2428